Enhancing Electric Vehicle Efficiency with a Novel SIMO DC-DC Converter: Integrating Multiple Speed Transmissions and Regenerative Braking

B Velliyangiri[1], R Dharaneesh[1], G Bala Surya[1], T Ragul kannan[1], K Boopathi[1]*

[1]Department of Mechanical Engineering, Nandha Engineering College, Perundurai 638 052, Tamilnadu, India

Abstract. An innovative single-input multi-output (SIMO) Direct Current (DC)-DC switched capacitor (SC) converter charged and discharged the flying capacitors by utilising one separate independent voltage source (Vbat or Vin) to control the EV's speed. The switching pulse interval remained constant, allowing for the generation of different voltage ratios. To regulate the velocities of EV, this study developed a number of speed transmissions. Utilising the SIMO DC-DC converter, the chosen and controlled battery voltage was produced. For motoring, or forwarding operation, four transmissions were used, while the other three transmissions were used for regenerative braking. A total of seven transmissions were generated by the proposed converter. Regenerative braking involved feeding the recovered voltage back into the battery, while the motor operated using energy from the fuel cell, photovoltaic cells, and the battery. Electronic add-ons like LED lights, the electric vehicle sound system, and charging ports for mobile devices and laptops all relied on the SIMO DC-DC converter. For various gear ratios, the suggested SIMO DC-DC converter used the energy restored in regenerative braking to recharge the battery. To further validate the proposed system, modelling, simulation, and analysis are employed. The 12 V fixed-voltage input and the 12 to 53 V output voltages are its intended uses. To ensure the system was reliable, it was simulated by the PSIM tool. Validation of the proposed converter provides strong proof of concept for regenerative braking and braking procedures.

1 Introduction

One important mode of transportation in recent years was the EV. The International Transport Forum predicted that CO_2 emissions will soar by almost 60% by 2050 as a result of the exponential growth of urban areas, leading to a worsening of the climate crisis. Concern over greenhouse gas emissions and the potential for EVs to help reduce these dangerous emissions [1]. Electric vehicles offered great promise for mitigating climate change. There are primarily two varieties of electric vehicles on the market. The first was the plug-in hybrid, or PHEV, which combined an electric motor with an internal combustion engine. A traction motor, batteries, power electronic controllers, and DC-DC converters are the four main parts of an EV. In a similar vein, smart vehicles are being created to out-do the standard electric vehicle [2]. Smart vehicles are currently controlled through the internet of things, and electric vehicles use both renewable and non-renewable energy sources as inputs. Furthermore, gear shift control, clutch control, and automatic transmission control are the major pillars upon which mechanical speed control was built and extensively researched [3, 4]. Electrical control was the fastest and most efficient way to control the speed transmission and regenerative braking. The speed of the E-vehicle was controlled in this work using a DC-DC speed control technique that was based on electricity [5, 6]. The DC-DC converter regulated the electric vehicle's speed and a number of other electrical components. The E-bike will be used as an example for the sake of clarity. A DC-DC converter was necessary for turning the DC motor on and off [7], 8]. Conventional converters had their limitations, namely electromagnetic interference (EMI) and losses of iron, but switched capacitors converters had many advantages, including high efficiency and the ability to achieve high target voltages with just switches and capacitors. Inductor-based converters, on the other hand, offer a better solution, but they also had their limitations. SC converters had many different uses. These SC DC-DC topologies were excellent for medium-and high-power applications as well. These DC-DC converters output was fed into DC-AC inverters, which efficiently convert DC power to AC voltage by using suitable PWM techniques to regulate the inverter [9, 10]. Through the use of medium-and high-power DC-DC converters, renewable energy sources are linked with grid. The SIMO SC DC-DC converter, a common topology in converters, was

* Corresponding Author: bvelliyangiri@gmail.com

© The Authors, published by EDP Sciences. This is an open access article distributed under the terms of the Creative Commons Attribution License 4.0 (https://creativecommons.org/licenses/by/4.0/).

considered for the aim of speed transmission. The DC-DC converter in an electric vehicle (EV) transformed the constant direct current (DC) power stored in the battery into variable direct current (DC), which was then used by different components in the circuit and driven a DC motor. The design of SC converter ensured that the negative current and voltage ripple are preserved [11]. The suggested speed control system's key benefit was that it regulated the vehicle's electronic components through acceleration and deceleration, as well as during motoring and regeneration. An additional feature that helped to increase the range of an EV was regenerative braking. In the regenerative braking cycle, the mechanical energy was converted into electrical energy [12]. Regenerative braking not only improved braking efficiency but also increased the driving range. Recent literature on regenerative braking covered a wide range of topics, but few of these studies addressed the topic of a fully automatic controller for a four-transmission system [13, 14]. This paper delves into a new four-transmission system that was designed for forwarding and regenerative operation. Fig.1 shows the regenerative braking technology that was part of the proposed system.

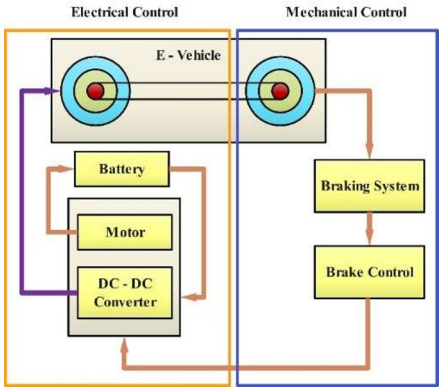

Fig. 1. The regenerative braking system's configuration

2 Proposed Method for Controlling Four-Transmission Converters

Fig. 2 shows the proposed SIMO DC-DC converter, which served as a switched capacitor connected in series and parallel around an oval route with a single source [15]. It consists of four flying capacitors and fourteen bidirectional switches (Vin or Vbat). To connect the many outputs (Vo1-Vo4) to the load, various output nodes were utilized. Transmission speed was proportional to the voltage ratio at each node, which was determined by connecting the output capacitor across every terminal. The converter that has been suggested was achieved step-up as well as step-down voltages. The voltage ratios (1 ∗ Vbat), (2 ∗ Vbat), (3 ∗ Vbat), (4 ∗ Vbat), (0.5 ∗ Vbat), and (0.33 ∗ Vbat) were produced by this converter that has been suggested. Table 1 shows the pulses for motoring and regenerative switching. There are two phases that driven the bidirectional switches, and their duty cycle ratio was 50%.

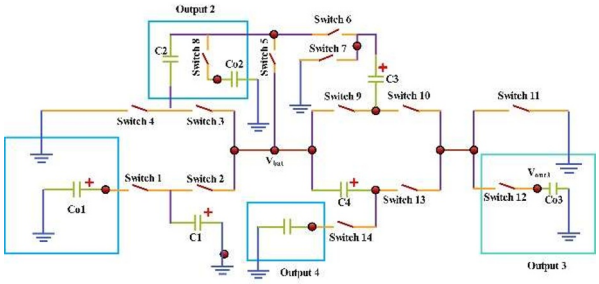

Fig. 2. The circuit of the proposed single-input multi-output Direct Current-DC converter

Phase (φ1) represented the charging state and the discharging condition was represented by phase (φ2). Various voltage ratios were generated by connecting the flying capacitor in parallel and series [16-18]. The details of the speed transmission switching were covered, and the transmission speeds were chosen in regard to the voltage ratios provided in Table 1. In this case, 12 V was taken as the input voltage, Vbat. Vo1 = 1 ∗ Vbat = 12 V was the output voltage for the first transmission. Also, the output voltage Vo4 for the fourth transmission was 53 V, which was equal to 4 ∗ Vbat. Various speed transmissions were generated by taking the following switching sequence into account. The concept of 3 ∗ Vbat speed transmission was used for the sake of simplicity. Activating switches S4, S5, S7, and S9 and parallel charging capacitors C2 and C3 with Vbat constitute Phase 1. In addition, in Phase 2, the secondary terminals of capacitor C2 and capacitor C3 were linked to the voltage source, and the capacitors are connected in series with Vbat. Switches S3, S6, S10, and S12 are used to connect the same terminal to C3. The operation modes of 3 ∗ Vbat are used in conjunction with capacitor C4 to produce transmission of 4 ∗ Vbat. The suggested converter allowed for regenerative braking to return energy to the battery. In Table 1, a half cycle with 50% positive (Pve), 50% negative (Neg), and an always-on switch are represented by the "Pve," "Neg," and "1," respectively.

Table 1. Speed transmission in switching pattern for both acceleration and deceleration

Speed Transmission	Switches (S)													
	1	*2*	*3*	*4*	*5*	*6*	*7*	*8*	*9*	*10*	*11*	*12*	*13*	*14*
Vbat	Pve	Neg	-	-	-	-	-	-	-	-	-	-	-	-
$2 \times V_{bat}$	-	-	Neg	Pve	Pve	Neg	Neg	-	-	-	-	-	-	-
$3 \times V_{bat}$	-	-	Neg	Pve	Pve	Neg	-	Pve	Pve	Neg	-	Neg	-	-
$4 \times V_{bat}$	-	-	Neg	Pve	Pve	Neg	-	Pve	Pve	Neg	Pve	Neg	Pve	Neg

3 Analysis and Operating Modes

An important factor to think about when constructing a SC converter was the equivalent resistance [19]. In order to keep things simple, the analysis uses voltage ratios of (4 ∗ Vbat). Two circuits of charging and discharging, shown in Fig. 3 and Fig. 4, represented the voltage ratio (4 ∗ Vbat). In any i[th] operational phase, the power loss [20] was given as

$$P_{R_{OUT_i}} = I_0^2 R_{\mathrm{OUT}_i} \quad (1)$$

Consider the following: Assume that the parasitic effects (ESR) and switch resistances on all flying capacitors are identical. Another point was that the filter capacitor capacitance (C1, C2, C3, C4) was much higher than the flying capacitor capacitance (C01, C02, C03, C04). Here was the current equation for phases φ1 and φ2, which was obtained by following the procedure, by performing nodal KCL analysis and using the charge balance equation in the manner depicted below [21]:

$$I_1 = I_2 + I_3 \quad (2)$$

$$I_4 = I_1 \quad (3)$$

$$I_4 = I_1 = I_0 \quad (4)$$

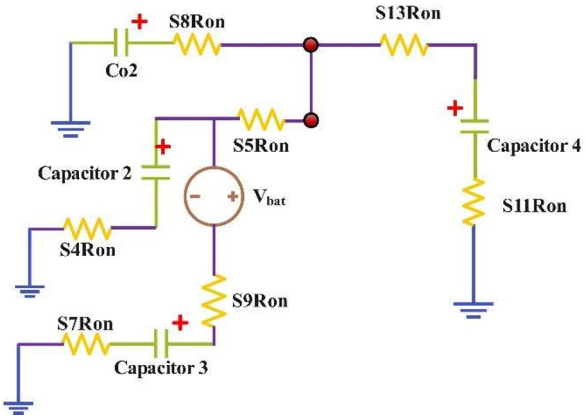

Fig. 3. Charging state equivalent circuit (4*Vbat)

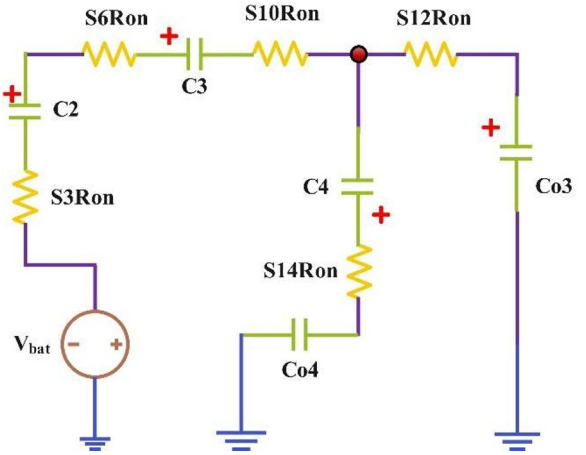

Fig. 4. The discharge state equivalent circuit is (4* Vbat)

Fig. 3 and Fig. 4 are used to derive the equation for charging the capacitor and discharging the capacitor, which was presented in (5)- (8).

$$R_C = \frac{1}{2}R_{\mathrm{on}} + \frac{1}{2}ESR \quad (5)$$

$$C_C = 2 * C \quad (6)$$

$$R_T = 4 * R_{\mathrm{on}} + 2 * ESR \quad (7)$$

$$C_T = \frac{C}{2} \quad (8)$$

Equation *Req*. [9] was derived by combining equations (5) to (8), and it was stated as

$$R_{eq} = \phi_c{}^2 \frac{1}{2f_s C_c} \coth\left(\frac{\lambda_c}{2}\right) + \phi_T{}^2 \frac{1}{2f_s C_T} \coth\left(\frac{\lambda_T}{2}\right) \quad (9)$$

For other voltage ratios, the same procedure was used to solve R_{eq}. Table 2 provided the R_{eq} of various voltage ratios.

Table 2. Four speed transmission's Equivalent resistance

Voltage Ratios	Model, R_{eq} (Ω)	Simulated, R_{eq} (Ω)
$1 * V_{bat}$	5.4	5.37
$2 * V_{bat}$	5.4	5.38
$3 * V_{bat}$	6.44	6.42
$4 * V_{bat}$	8.18	8.17

4 Simulation and Discussions

Using preexisting mechanical braking systems, this study merely designed the electrical speed transmission control [22]. Using Fig. 2 as a reference, the factors of the MAX4678 switches, $S_1 - S_{14}$ are $R_{on} = 0.4\Omega$, and the PSIM tool was utilized to simulate and validate the proposed converter. For the various voltage ratios, the load current was range between 2 mA to 1 A at 12 V. The output capacitor and flying capacitor had ratings of 220 μF and 22 μF, respectively, including an ESR of 100 mΩ and 5kΩ, and the load current was range between 2 mA to 1 A at 12 V. Table 3 displayed the results of comparing the model (V_m), the simulated (V_{out}), and the theoretical voltages (V_o) of the voltage ratio. The following scenarios are used to run the simulations:

Case 1: The electronic loads are linked to the converter outputs designated as ($V_{o1} - V_{o4}$).

Case 2: The electric vehicle (EV) load was linked to one of the outputs, while the electronics load was linked to the remaining outputs.

Case 3: Voltage that was used for regeneration is fed back into the V_{bat}.

Case 4: Every load was linked to the motor through V_{bat}, and the regenerative voltage was returned to V_{bat}.

Table 3. The outcomes of comparing the speed transmission of V_{om}, V_{rat}, and Vo

Frequency (kHz)	Voltage Ratios	Analysis, V_{om} (V)	Model, V_{rat} (Vrat)	Simulated (Vom)
100	$1 * V_{bat}$	16.16	16.21	16.16
100	$2 * V_{bat}$	29.02	29.07	29.02
100	$3 * V_{bat}$	39.34	39.38	39.34
100	$4 * V_{bat}$	52.20	52.25	52.20

4.1 Case 1

Here, every load on the proposed converter was connected to the electronic load. Fig. 5 displayed the voltage ripple with output voltage of the 4 * Vbat voltage ratio, which was 0.1 V. As demonstrated in Fig. 6, the model values and each of the simulated output voltages were nearly same. Fig. 7 shown the simulated output voltage in 3 * Vbat, which was 39.38 V. Also, it was cleared that this voltage was very close to the model voltages. Changing the value of resistance between 1 kΩ and 5 kΩ in the voltage ratio 4 * Vbat shown the variation of load in proposed converter depicted in Fig. 5. The proposed converter was based on results of (Vo), (Vm), and (Vout) values that are highly concordant with one another.

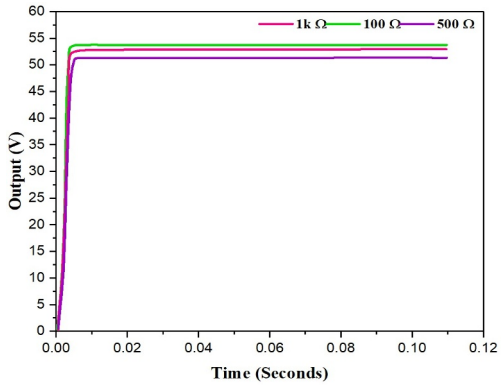

Fig. 5. A simulated output voltage of 4*Vbat under different loads

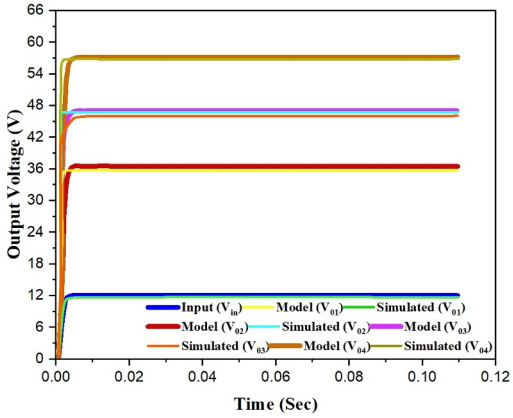

Fig. 6. Single Input Multi Output Direct Current-DC converter simulation and model voltages

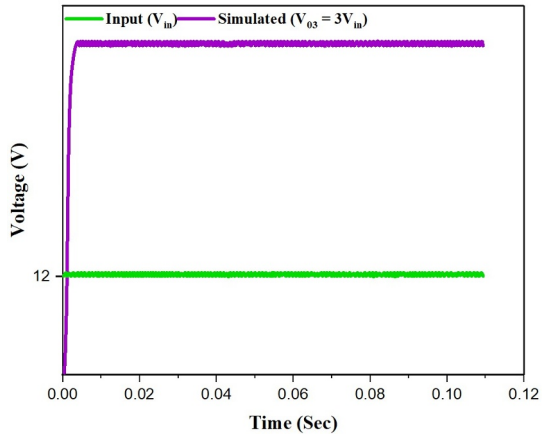

Fig. 7. Voltage output simulation for SIMO in 3*Vbat mode

4.2. Case 2

The basic E-bike's ranges were used to assume the current, torque, and speed parameters. When developing the parameters of the E-vehicle, certain assumptions were made. This bike had the following specs: a 3 kg motor/gear, a 0.5 kg controller, a 3 kg battery, and a 10 kg rider. Consider the current values of the following parameters for a bicycle: Vb = 5 km/h, Fd = 13 Nm, head wind speed = 1 km/h, Pd = 18 W, and Pd = 20 W (with an additional 2 W for propulsion). Consideration of real-time factors was made during the design of the electric vehicle. The EV's power and torque should not be assumed. Connecting the load to the motor caused the suggested converter to produce a simulated output voltage, as shown in Fig. 8. At 14.25 RPM, 12 V input, 13.6 Nm torque, 11.98 V output, and 2.05 A load current, it produced efficient results. This proved that the suggested converter still delivers efficient operation even with the motor load attached.

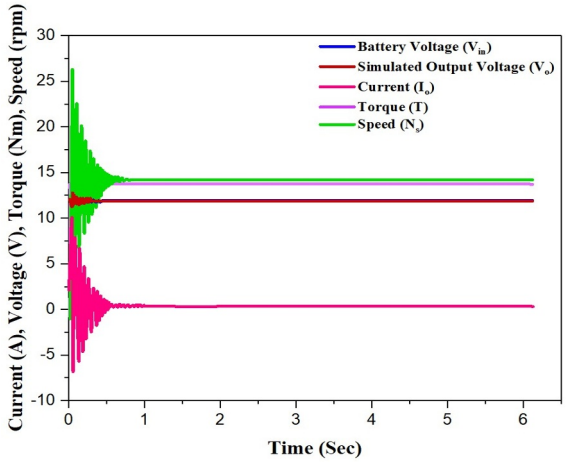

Fig. 8. An output voltage that is generated when a DC motor is used as a load

4.3 Case 3

During regenerative braking, the electric vehicle's energy was returned to its source through the use of the same converter that was suggested. This converter will charge the battery using various step-down voltage ratios, creating a buck operation. Table 4 shown the on and off switching pulse pattern for the regenerative system, and for the sake of simulation and analysis, let's use (0.3 * Vout) voltage ratios for the regenerative voltage. Assuming the regenerative voltage was not reached, the desired voltage Vbat should be approximately 12 V (12 V battery charging at a predetermined voltage). For battery charging, the Single Input Multi Output converter chosen between various voltage ratios. The suggested converter's simulated output voltage in regenerative braking was shown in Fig. 9.

Table 4. Analysis of the suggested converter's regenerative switching pattern

Speed Transmission	Switches (S)													
	1	2	3	4	5	6	7	8	9	10	11	12	13	14
$1 \times V_{bat}$	Neg	Pve	-	-	-	-	-	-	-	-	-	-	-	-
$0.5 \times V_{bat}$	-	-	-	-	-	Neg	1	-	Neg	Pve	Neg	-	Neg	Pve
$0.33 \times V_{bat}$	-	-	-	1	Neg	Pve	Neg	-	Neg	Pve	Neg	-	Neg	Pve
$0.25 \times V_{bat}$	1	-	Pve	Neg	Neg	Pve	Neg	-	Neg	Pve	Neg	-	Neg	Pve

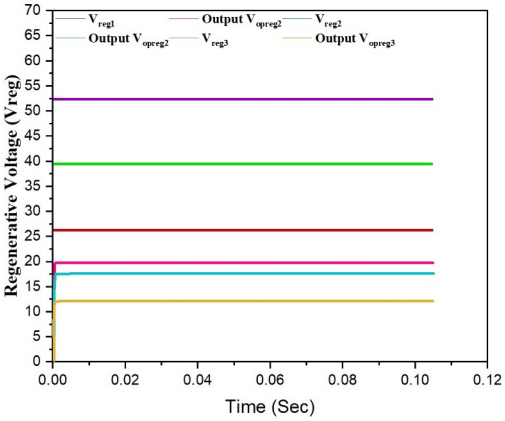

Fig. 9. Regenerative braking simulation output voltage

The overall efficiency of the suggested converter for both regenerative braking and motoring was illustrated in Fig. 10. Table 5 presented a comparative analysis of several factors in relation to previous research studies [23, 24]. The outcome was more efficient converter with reduced voltage ripple, fewer switches, and capacitors. Without modifying the circuit design, the proposed converter could also function in regenerative mode in addition to forwarding mode. As illustrated in Fig. 10, the SC converter boasted impressive efficiency when operating in open-loop conditions in this simulation. Consequently, the suggested system for manual transmission does not necessitate the closed-loop system. When it comes to Case 3, automatic switching might be improved with closed-loop operation for speed and efficiency.

Table 5. Evaluation outcomes of SC speed controller converters

Voltage Ratios	Number of				Regenerative
	Capacitors	Switches	Inputs	Outputs	
10	4	14	1	4	Yes

4.4 Case 4

Here, the motor load was linked to each of the output terminals, which had varying ratings. The motor terminals were used to connect all the loads, and as shown in Fig. 11, Additionally, these terminals were utilized for regenerative braking to return power to the battery [25]. The output 1 voltage was depicted in Fig. 11a. In case 4, the same motor parameters are used. The output voltage and the model voltage were nearly identical in Fig. 11a. Output 1 Vbat voltage was 12 V, calculated as 1 * Vbat. Voltages of 24 V, 36 V, and 43 V were also provided by the other outputs. The similarity between the model voltage and the vast majority of the output voltages was depicted in Fig. 11(a) to Fig. 11(d). Fig. 11 also shown that the motor speed was adjusted based on the suggested converter voltage. In this case, the torque remained constant regardless of the circumstances. Fig. 11 shown that the suggested system could control the torque and speed of all terminals without affecting the system's efficiency or speed, even when parallel connections are made between each output port and the motor points.

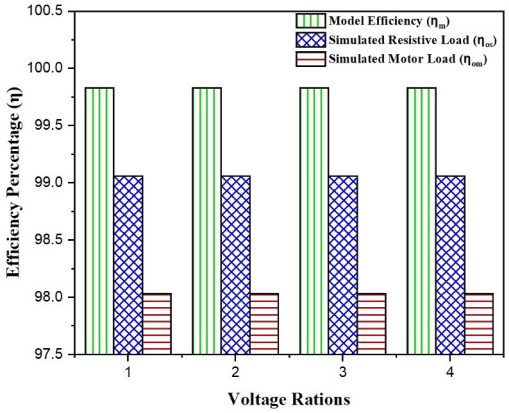

Fig. 10. The proposed converter's efficiency

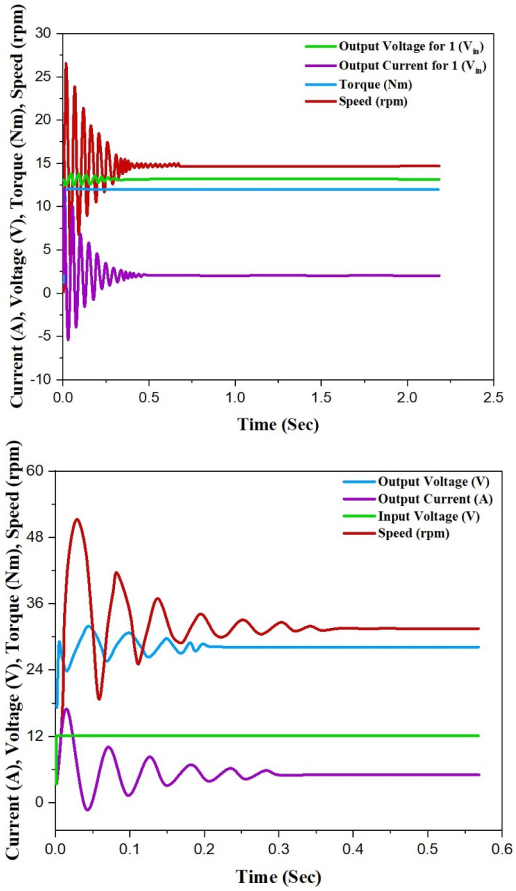

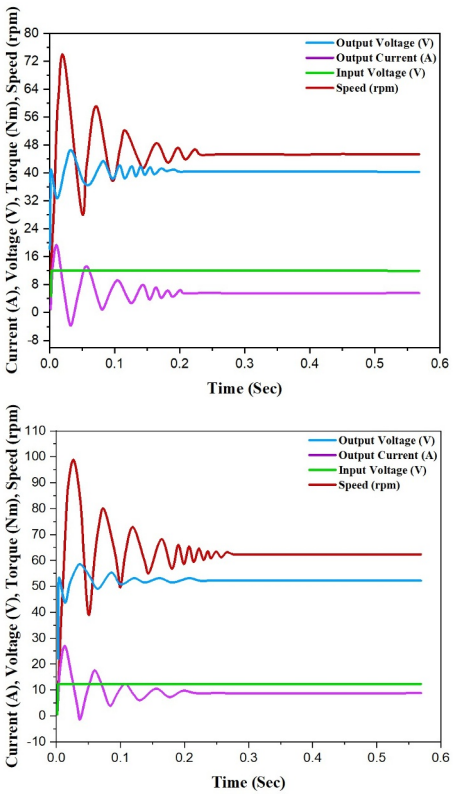

Fig. 11. Parallel connected simulation results of SIMO DC-DC converter are displayed. (a) Output voltage **for 1** $* V_{bat}$. (b) Output voltage **for 2** $* V_{bat}$. (c) Output voltage **for 3** $* V_{bat}$. (d) Output voltage **for 4** $* V_{bat}$.

5 Experimental Results and Discussions

The proposed converter's prototype is depicted in Fig. 12. Limitations in the switching parameters caused the input voltage to be nearly 5 V. Various conversions' regenerative and forward voltages were displayed in Fig. 12(b) to Fig. 12(d). Based on these findings, it appeared that the simulation and hardware outcomes are nearly identical. Research into loading and unloading was still in its early stages. The proposed converter is validated with the help of the prototype. This converter application is designed for electric vehicles. The purpose of this prototype was to test the converter in a controlled environment. It evident from Fig. 12 that the suggested prototype model for the Single Input Multi Output DC-DC converter yields satisfactory results when compared to the simulation outcomes. Furthermore, future research will determine whether the same converter can be utilized for electric vehicle applications.

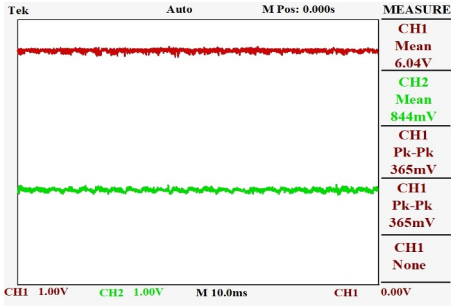

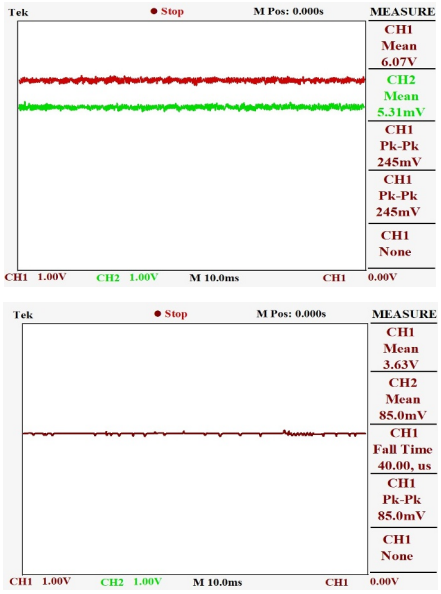

Fig. 12. Results from Single Input Multi Output DC-DC converter experiment. (a) The prototype of Single Input Multi Output Direct Current-DC converter. (b) Voltage forwarding of Vbat. (c) Voltages of 4Vbat for forwarding and regeneration

6 Conclusions

Electric vehicles (EVs) can achieve greater acceleration and deceleration with the help of the suggested speed transmission system. Regenerative braking employs acceleration or deceleration to recharge the battery; it was controlled by the transmission control as well. To further guarantee that the suggested system provides maximum efficiency and effective braking actions, modelling, simulation, and analysis are employed. Eleven switches and four capacitors make up the design of the four-transmission speed control. With the bicycle load, the suggested system achieved an efficiency of over 90% at 13 RPM and 15 Nm of measured torque. Not only that, but the suggested converter has dual compatibility with battery and fuel cell systems. The key benefits of this system were that it could use various capacitor charging operations and switching patterns to achieve transmission speeds that were one to three times the input voltage.

References

1. Z. Cabrane, S. H. Lee, Control and Management of Railway System Connected to Microgrid Stations. IEEE Access. **10,** (2022).
2. D. Chandran, A. Haseena, K. Biju, Multi-input Single-Output Superboost DC-DC Converter for Solar-Powered Electric Vehicle. in Lecture Notes in Electrical Engineering. (2023).
3. S. Manjare, S. Saraf, C. Rajeshwari, Design and Control of Bidirectional Converter for EV Application, in 2023 IEEE Renewable Energy and Sustainable E-Mobility Conference, RESEM, (2023).

4. S. K. Singh, D. Kumar, M. Prakash, A. Kumar, P. K. Sadhu, Analysis and Control Implementation for Instantaneous Mode Switching Bi-Directional Dc-Dc Converter for Plug-In Electric Vehicle, in Second International Conference on Energy, Power and Environment: Towards Smart Technology, ICEPE (2018).
5. K. V Anandkrishnan, S. Suresh Kumar, T. T. Anilkumar, P. Jayaprakash, Fuel Cell - Battery Integrated BLDC Motor for Electric Vehicle with Regenerative Braking, in IEEE 19th India Council International Conference, INDICON, (2022).
6. H. Assem, T. Azib, F. Bouchafaa, A. Hadj Arab, C. Laarouci, Limits control and energy saturation management for DC bus regulation in photovoltaic systems with battery storage. Solar Energy. **211,** 2020.
7. M. Vairavel, R. Girimurugan, C. Shilaja, G.B. Loganathan, J. Kumaresan, Modeling, validation and simulation of electric vehicles using MATLAB. In AIP Conference Proceedings. **2452,** (2022).
8. R.K.G. Radhakrishnan, U. Marimuthu, P.K. Balachandran, A.M.M. Shukry, T. Senjyu, an intensified marine predator algorithm (MPA) for designing a solar-powered BLDC motor used in EV systems. Sustainability. **14,** (2022).
9. B. M. Manjunatha, D. V Ashok Kumar, M. Vijaya Kumar, A simplied PWM technique for isolated DC-DC converter fed switched capacitor multi-level inverter for distributed generation. International Journal of Power Electronics and Drive Systems. **8,** (2017).
10. C.-H. Huang, A. Mandal, D. Pena-Colaiocco, E. P. D. Silva, V. S. Sathe, Regenerative Breaking: Optimal Energy Recycling for Energy Minimization in Duty-Cycled Domains. IEEE J Solid-State Circuits. **58,** (2023).
11. M. Vairavel, R. Girimurugan, C. Shilaja, C., G.B. Loganathan, G.B. Z. Polat, Analysis of hybrid electrical vehicles: Types, formulation and needs. In AIP Conference Proceedings. **2452,** (2022).
12. T. Jitson, M. Vongkulbhisal, S. Cheapanich, Regenerative Battery Charging Control for PMDC Motor Using a Modulus Counter Switching Technique, in Proceedings of the 2022 International Electrical Engineering Congress, iEECON, (2022).
13. L. Malafronte, M. Grandone, A. Lega, M. Pennese, C. Pianese, Modelling and Control of a Novel Clutchless Multiple-Speed Transmission for Electric Vehicles. in SAE Technical Papers. (2019).
14. T. Farjam, M. S. Foumani, M. Delkhosh, Optimization of multiple transmission layouts for minimal energy consumption of a battery electric vehicle. Scientia Iranica. **26,** (2019).
15. C. Li, F. Meng, J. Xi, Y. Zhai, Starting shift control of heavy-duty automatic transmissions based on the optimal trajectory of turbine speed. Mech Syst Signal Process. **126,** (2019).
16. Yadav and S. K. Maurya, Modelling and Analyzing of dc to dc Converter for Solar Pump Applications, in International Conference on Power Electronics and IoT Applications in Renewable Energy and its Control, PARC, (2020).
17. M.D. Sreehari, K. Manikandan, K. Pranjith, V. Adithya, M.B.J. Ram, V. Indu, M.M. Dharmana, Design and Analysis of E-Bike with Electrical Regeneration and Self-Balancing Assist, In Fourth International Conference on Trends in Electronics and Informatics ICOEI, (2020).
18. M. Liao, D. H. Zhou, P. Wang, M. Chen, Power Systems on Chiplet: Inductor-Linked Multi-Output Switched-Capacitor Multi-Rail Power Delivery on Chiplets, in Fourth International Symposium on 3D Power Electronics Integration and Manufacturing, 3D-PEIM (2023).
19. J. Hong, D.-W. Zhang, G.-P. Wang, S. Ni, Simulation of a regenerative braking system producing controlled braking force. in Advanced Materials Research. (2012).
20. S. Suresh, C. N. Raghu, R. Dash, J. R. Kalvakurthi, S. Athikkal, V. Subburaj, SIMO DC-DC Converter for E-Vehicle and Regenerative Braking Based on Simulation and Model Investigation. Energies (Basel). **15,** (2022).
21. M. R. Rade, J. A. Mane, O. N. Buwa, Performance Evaluation of Electric Vehicle Using Hybrid Energy Storage System. in Lecture Notes in Electrical Engineering. (2022).
22. S. Saahithi, B. Hemanth Kumar, K. Jyotheeswara Reddy, R. Dash, V. Subburaj, Four Speed Auto Transmission DC-DC Converter Control for E-Vehicle and Regenerative Braking Based on Simulation and Model Investigation. Distributed Generation and Alternative Energy Journal. **38,** (2023).
23. K. Sayed, Zero-voltage soft-switching DC-DC converter-based charger for LV battery in hybrid electric vehicles. IET Power Electronics. **12,** (2019).
24. X. Jia, C. Hu, S. Du, M. Chen, P. Lin, D. Xu, DC-link voltage control strategy of a bi-directional DC/DC converter for electric vehicles, in IEEE Energy Conversion Congress and Exposition, ECCE, (2015).
25. V. Shah, S. Payami, A Multi-Level Converter for SRM Drive Based EV Applications with Auxiliary Load Driving Capability, in Second IEEE International Conference on Sustainable Energy and Future Electric Transportation, SeFeT, (2022)